



ELSEVIER

Journal of Molecular Catalysis A: Chemical 162 (2000) 227–246



www.elsevier.com/locate/molcata

Structural and catalytic properties of sodium and cesium exchanged X and Y zeolites, and germanium-substituted X zeolite

P. Concepción-Heydorn¹, C. Jia, D. Herein², N. Pfänder, H.G. Karge, F.C. Jentoft*

Department of Inorganic Chemistry, Fritz-Haber-Institut der Max-Planck-Gesellschaft, Faradayweg 4-6, 14195 Berlin, Germany

Abstract

The conversion of isopropanol in a fixed bed flow reactor was used as a test reaction for a number of faujasite-type zeolites which were modified in order to increase their basicity. Samples included a CsY zeolite with an intact faujasite structure and an exchange degree of nearly 100% prepared by solid-state ion exchange, a CsNaY obtained from CsY through exchange with aqueous NaCl solution, a CsNaX obtained from NaX and aqueous CsCl solution, and a Na(Ge)X, with Si replaced by Ge. At 623 K, an isopropanol partial pressure of 5 kPa in He, and a total feed flow of 90 ml/min, a catalyst mass of 50 mg, initial yields were as follows: NaY: 62% propene, CsNaY: 78% propene, NaCsX: 10% propene, 0.37% acetone, Na(Ge)X: 8% propene, 11% acetone. Conversion in the presence of CsY was < 1%. CO₂ adsorption and infrared (IR) spectroscopy were used to probe basicity, and Na(Ge)X was the only sample to form monodentate carbonates upon CO₂ adsorption (bands at 1477 and 1428 cm⁻¹). Further characterization with X-ray diffraction (XRD), transmission electron microscopy (TEM), thermal analysis, nitrogen sorption, and isopropanol sorption was necessary to properly interpret catalytic results by identifying samples which contained impurities, had blocked pore systems, or decomposed partially during activation or reaction. © 2000 Elsevier Science B.V. All rights reserved.

Keywords: Alkali metal cation exchanged faujasite-type zeolites; Isopropanol dehydrogenation; Infrared spectroscopy; X-ray diffraction; CO₂ adsorption

1. Introduction

The advantages associated with the use of zeolites as catalysts would make it desirable to expand their application to base-catalyzed reactions. The constitu-

tion of zeolites leads to acidic rather than basic properties, i.e. the negatively charged zeolite frameworks create Brønsted acidic sites. Zeolites with a positively charged framework which would provide Brønsted-basic OH groups are not known [1]. Two principal methods to create and enhance basicity in zeolites have been proposed and investigated [1], i.e. (i) the more or less trivial use of the zeolite as a support for basic species, i.e. the occlusion of metal (alkali) clusters, or small metal hydroxide and/or oxide particles, and (ii) modification of the intrinsic basicity of the zeolite, i.e. the Lewis basicity of the

* Corresponding author.

E-mail address: jentoft@fhi-berlin.mpg.de (F.C. Jentoft).

¹ Current address: Instituto de Tecnología Química, Universidad Politécnica de Valencia, 46071 Valencia, Spain.

² Current address: Institut für Angewandte Chemie Adlershof e. V., Richard-Willstätter-Straße 12, 12489 Berlin, Germany.

framework oxygens, by either using different framework cations (isomorphous substitution), or by exchange of the cations that balance the charge of the framework. Specifically, as charge balancing cations, low electronegativity cations such as alkali metal cations appear suitable; and in zeolites of the faujasite-type alkali metal cations can be introduced into the supercages by means of ion-exchange in an aqueous solution of a salt of the desired cation (referred to hereafter as conventional ion exchange).

X and Y zeolites that have been modified through conventional ion exchange with alkali metal cation solutions indeed exhibit basic properties useful for catalysis, as shown by their effectiveness for various test reactions which include side-chain alkylation of toluene [2–8], the *N*-alkylation of aniline [9,10], the dehydrogenation of isopropanol or other alcohols [11–13], Knoevenagel condensations [14,15], and double bond isomerizations [16,17]. A number of trends have been observed in the catalytic activities of such samples but these trends are not entirely consistent. Investigations on toluene alkylation have shown that the yield of the side chain alkylation products styrene and ethylbenzene, indicative of base catalysis, could be correlated with the intermediate Sanderson electronegativity (S_{int}) [5]; the formation of these products becomes significant at $S_{\text{int}} < 3.6$. The yield of styrene and ethylbenzene was found to increase with increasing cation size, i.e. in the order $\text{Na} < \text{K} < \text{Rb} < \text{Cs}$, except for CsX due to stability problems, and X zeolites were found to be more active than Y zeolites [3]. Sefcik [18] investigated the rotational freedom of aromatics adsorbed on modified zeolite X with nuclear magnetic resonance spectroscopy and concluded that cations as large as Cs^+ in the supercages sterically hinder ring alkylation while the side chain can be alkylated. Engelhardt et al. [4] found that NaX, KX, and CsX that were obtained through exchange with alkali metal hydroxides were more active than samples obtained with other alkali metal salts, concluding that small amounts of occluded hydroxides have a positive effect.

Investigating the reaction of isopropanol [19,20] where dehydrogenation to acetone indicates the presence of strongly basic sites, with cation exchanged X and Y zeolites as catalysts [35], Yashima et al. [19] found that the yield of acetone increased with cation

size, but for this reaction, Y zeolite was more active than X zeolite when the cation was K, Rb, or Cs. Jacobs and Uytterhoeven [13] suggested that the rate of acetone formation was related to the concentration of iron impurities rather than to the alkali metal cation radius. Hathaway and Davis [20] used various alkali metal salts for the conventional ion exchange, investigated the resulting zeolite samples in an unrinsed and a rinsed state, and performed not only the isopropanol test reaction but also chemical and spectroscopic analysis of the materials to identify occluded species. Unrinsed samples prepared from alkali metal acetates and hydroxides were more active for acetone formation than samples prepared from alkali metal nitrates, and samples prepared from alkali metal chlorides were entirely inactive for isopropanol dehydrogenation. Catalytic activity was, at least in part, attributed to occluded salts, whose presence was confirmed by infrared (IR) spectroscopy and chemical analysis which sometimes revealed a cation excess ($n_{\text{M}^+}/n_{\text{Al}} > 1$). Unrinsed zeolites Y with potassium or cesium, prepared from hydroxides, had a higher rate of formation of acetone and a higher selectivity for acetone than the corresponding zeolite X samples. Rinsing the samples with deionized water increased the activity towards propene formation, which was explained with re-exchange of alkali metal cations by protons.

The strength of basic sites in zeolites that have been modified with alkali metal salts has been investigated using the adsorption of probe molecules in combination with various methods, e.g. the adsorption of pyrrole in combination with IR spectroscopy [21,22], or X-ray photoelectron spectroscopy (XPS) [23], or the adsorption of carbon dioxide in combination with IR spectroscopy [11], microcalorimetry [16], or temperature-programmed desorption (TPD) [24,25]. Barthomeuf [26] derived from IR spectra taken after adsorption of pyrrole that the basic strength of the framework oxygen increases depending on the cation in the order $\text{Na} < \text{K} < \text{Rb} < \text{Cs}$. For any given cation, the basicity was found to increase with increasing Al content [26], consistent with IR measurements by Scokart and Rouxhet [21] who adsorbed pyrrole on NaY and NaX. XPS spectra of the N1s level of adsorbed pyrrole [23] and the Cl2p level of adsorbed chloroform [27] confirm the ranking of alkali metal cations and also show X

zeolite to be more basic than Y zeolite. Doskocil and Davis [11] investigated carbonate species formed upon CO₂ adsorption and their thermal stability with IR spectroscopy; the results indicated that KX had stronger basic sites than CsX. Laspéras et al. [24] concluded from TPD measurements that CO₂ adsorption cannot be related to framework basicity but rather to cation polarizing power. Occlusion of cesium oxide in alkali metal cation exchanged zeolites created basic sites [11,16,24,25]. Direct spectroscopic measurements of the negative charge on the framework oxygen with XPS by Okamoto et al. [28] showed that the charge increases with increasing Al content and with an increasing fraction of Na replaced by Cs in NaY.

Heidler et al. [29] used the electronegativity equalization method to calculate the negative charges on the framework oxygens of faujasite, which on average increased with increasing Al content. The oxygen atoms in the supercages were identified as the most basic, and their negative charge was enhanced in high aluminum content ($n_{\text{Si}}/n_{\text{Al}} = 1$) faujasites when sodium on sites II and III was replaced by cesium.

In summary, some trends evolve for the properties of alkali metal cation exchanged faujasites obtained through conventional ion exchange. The basicity increases with decreasing electronegativity of the alkali metal cation. Zeolite X exhibits higher basicity but apparently lower stability than zeolite Y. An obvious problem arises from occluded basic species, which potentially obscure the identification of framework basicity, and at the same time reduce the accessibility of the pore system. The detection of such occluded species requires characterization beyond bulk chemical analysis, which can only give a hint of occluded species in cases where a cation excess is found. Moreover, the exchange degree, as obtained from chemical analysis, may not account for occluded species. The exchange degrees in the discussed papers vary greatly, e.g. from 44% (RbX [27]) to 98% (KY [26]), and specifically for the Cs cation from 51% to 77% (X zeolite) and 63–80% (Y zeolite) [3,19,20,23,26,27]. Cation excess in the samples discussed above reached 12% to 23% [20].

One of the goals of this work was to use solid-state ion exchange [30–32] in order to prepare samples with a high degree of exchange (> 95%). Although

the sodalite cages are not accessible for most reactants, the cations in these cages may still influence the basicity of oxygens pointing into the supercage. It may thus be possible to further increase basicity; an increase in the basicity of framework oxygens upon exchange of protons by cations of low electronegativity can be postulated based on Sanderson electronegativity estimates [1]. In the case of high degrees of exchange, another obstacle, i.e. the migration of cations [33,34] between the positions in the hexagonal prisms, the sodalite cages, and the supercages which may happen during dehydration, adsorption of probes, or reaction, would be of no effect.

Alkali metal chlorides are used in this work for the ion exchange, so that there is no danger of producing a basic alkali metal oxide as from oxygen containing precursors. Unrinsed samples prepared from chlorides in conventional ion exchange were found inactive [20]. Our focus is on cesium, which is expected to have the largest effect on the basicity. X and Y zeolites are investigated in an attempt to resolve the question of their different basicity and stability. An isomorphously substituted zeolite, Na(Ge)X, with a near-faujasite structure, germanium in the place of silicon, and a Ge/Al ratio of 1, which was shown to be active for base-catalyzed reactions in previous experiments [14] is included for comparison purposes. X-ray diffraction (XRD) and transmission electron microscopy (TEM) are used to confirm the structural integrity of the framework after the exchange. Carbon dioxide, which can form carbonates with basic oxygen atoms, was used as a probe and its adsorption was followed by IR spectroscopy. The conversion of isopropanol [35] was used as a test reaction, and the stability and regenerability of the catalysts was also tested.

2. Experimental

2.1. Preparation

The NaY parent sample was obtained from Degussa, Hanau, Germany ($n_{\text{Si}}/n_{\text{Al}} = 2.8$, manufacturer's information). NH₄Y was obtained by 20 times repeated ion exchange of the NaY zeolite with a 1 N

NH₄Cl solution at 345 K. The ion exchange degree was 95% (atomic absorption spectroscopy [AAS]). “CsY” zeolite was obtained by solid-state reaction of CsCl salt (Merck, Darmstadt, dried at 355 K, 1 h) and NH₄Y with a molar ratio $n_{\text{Cs}}/n_{\text{Al}} = 1.1$. A mixture of CsCl and NH₄Y was prepared with a suspension method employing hexane as solvent (38.05 g NH₄Y, 23.22 g CsCl, 80 ml hexane). The suspension was stirred at room temperature (RT) until the hexane was completely evaporated. The mixture of NH₄Y/CsCl was heated in vacuum to 440 K (2.5 K/min) and maintained at 440 K for 20 h, then the temperature was increased to 725 K (2.5 K/min), and the sample was kept at this temperature for 20 h. The sample was heated again in a quartz tube under high vacuum up to 415 K (5 K/min) and kept at this temperature for 20 h. Then the temperature was increased with 2 K/min up to 725 K, and maintained at 725 K for 20 h. A fraction of the sample was washed by stirring it in a 0.2 M Cs₂CO₃ aqueous solution at RT for 24 h. This sample was filtered and dried at 393 K and is designated CsY-

washed. “CsNaY” was prepared by re-exchange of CsY with NaCl aqueous solution (1 g CsY in 50 ml 0.02 M NaCl) at RT for 24 h. The sample was filtered, washed with distilled water, and dried at 393 K. “CsNaX” (~ 50% Cs) and “Na(Ge)X” were kindly provided within the EU Human Capital and Mobility — Scientific and Technical Cooperation Network. CsNaX was prepared by suspending and stirring NaX in 2 M CsCl solution in water at 353 K for 1 h. The resulting material was filtered from the solution and the procedure was repeated twice with fresh solution. Na(Ge)X was prepared following the procedure of Lerot et al. [36], i.e. in a hydrothermal synthesis at 363 K starting from metallic aluminum and germanium dioxide dissolved in sodium hydroxide solution.

2.2. Characterization

Thermogravimetry (TG)/DTA experiments were conducted in a TG/DTA 320, Seiko Instruments,

Table 1

Chemical composition data from AAS, SEM–EDX, TEM–EDX; weight loss data (TG); N₂ (77 K) and isopropanol (353 K) sorption data

Sample	Si/Al (Ge/Al)	Cs/Al	Weight loss from RT to 823 K (wt.%)	Apparent surface area from N ₂ sorption capacity (m ² /g of dry zeolite)	N ₂ sorption (mol/u.c.) ^a	Pore volume from N ₂ sorption at $p/p_0 = 0.3$ (ml/g of dry zeolite)	Isopropanol sorption capacity at 300 Pa/353 K (mol/u.c.) ^a
NaY	2.92 2.80 ^b	–	22	580	76	0.28	47
CsNaY	2.85 2.95 ^c 2.79 ^d	0.79 0.57 ^c 0.89 ^d	15	348	60	0.18	33
CsY non-washed	2.65 2.90 ^c 2.53 ^d	1.26 1.14 ^c 1.29 ^d	10	144	28	0.08	18
CsY washed	2.84 2.96 ^c	1.19 0.97 ^c	12	273	52	0.13	–
NaCsX	1.28	0.57	17	404	75	0.19	–
Na(Ge)X	1.10 ^d	–	20	217	40	0.10	–

^aThe following idealized u.c. were used for the calculation: Na₅₄(SiO₂)₁₃₈(AlO₂)₅₄, Cs₃₈Na₁₆(SiO₂)₁₃₈(AlO₂)₅₄, Cs₅₄(SiO₂)₁₃₈(AlO₂)₅₄, Cs₄₂Na₄₂(SiO₂)₁₀₈(AlO₂)₈₄, Na₉₆(GeO₂)₉₆(AlO₂)₉₆.

^bManufacturer’s information.

^cFrom SEM–EDX.

^dFrom TEM–EDX.

and ca. 10 mg of sample were heated in air with a heating rate of 5 K/min. TEM was performed with a Philips CM 200 FEG with a 200 keV electron beam, equipped with an EDAX DX4 accessory for energy dispersive X-ray (EDX) analysis. Scanning electron microscopy (SEM) was performed with a SEM Hitachi S-4000-FEG with a 5–25 keV incident beam, equipped with an EDAX DX4 accessory. Diffractograms were recorded in focussing Debye–Scherrer geometry, using a Stadi P diffractometer (STOE & CIE), Cu K α 1 radiation ($\lambda = 154.06$ pm), a curved Ge primary monochromator, and a linear PSD with a maximum resolution of $2\theta = 0.01^\circ$. Samples were filled into 0.5-mm Lindemann capillary tubes.

Nitrogen adsorption measurements were performed with an Autosorb-1 (Quantachrome) at 77 K. Samples were heated with 5 K/min to 453 K, kept for 2 h at 453 K, then heated to 673 K with a rate of 1 K/min, kept for 4 h at 673 K, and cooled down to 77 K. Isopropanol adsorption isotherms were recorded in a volumetric apparatus [37] at 353 K

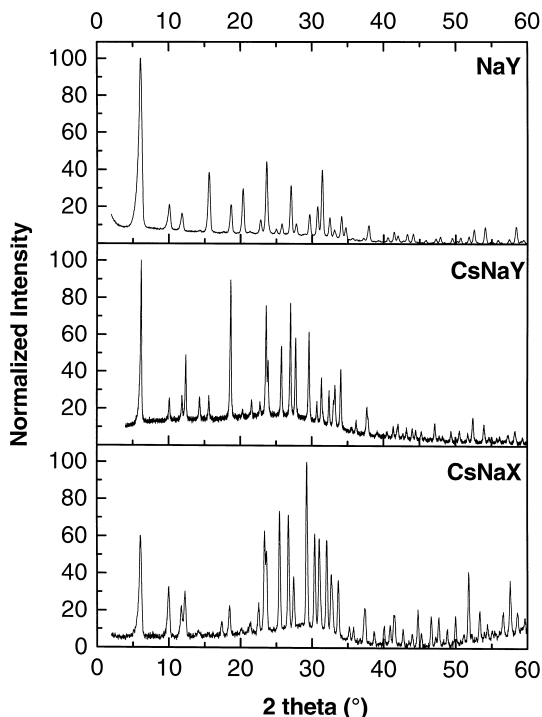


Fig. 1. X-ray diffractograms of NaY (top); CsNaY (middle); and CsNaX (bottom).

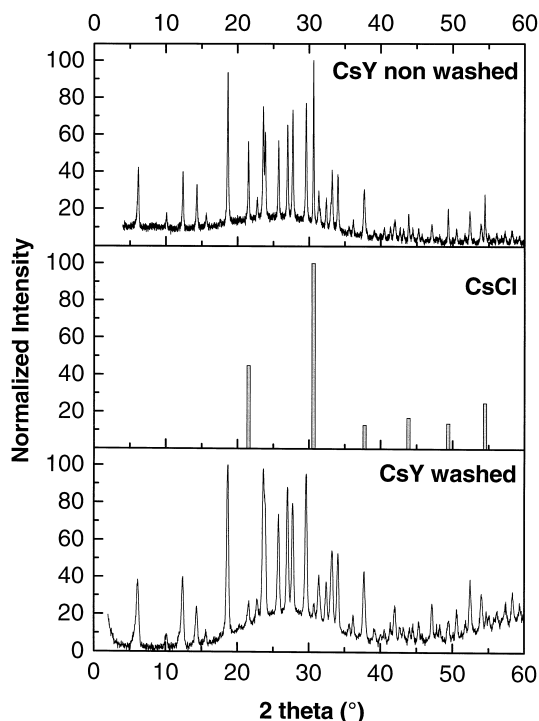


Fig. 2. X-ray diffractograms of CsY (top); CsCl reflections added from database (middle); and CsY-washed (bottom).

after pretreating the samples at 623 K in vacuum ($\approx 10^{-5}$ hPa) for 5 h.

IR measurements were performed with a Perkin-Elmer System 2000 FTIR spectrometer. Samples

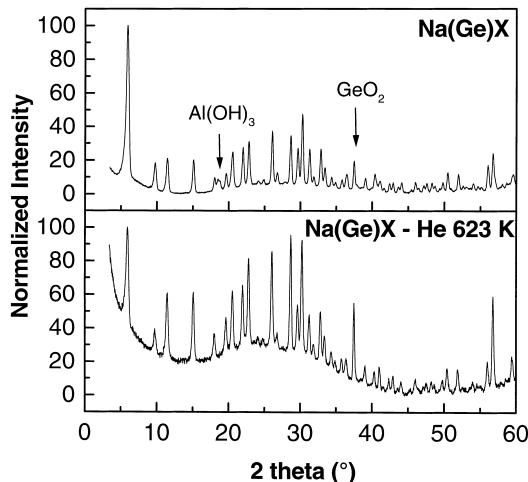


Fig. 3. X-ray diffractograms of Na(Ge)X as received (top); and after treatment at 623 K in flowing He (bottom).

were pressed into self-supporting wafers ($2.5\text{--}6\text{ mg/cm}^2$) and introduced into a transmission IR cell (CaF_2 windows). Pretreatment was performed stepwise with a heating rate of 5 K/min and a holding time of 2 h at 473 , 573 , 673 , 773 K . $\text{Na}(\text{Ge})\text{X}$ was heated straight to 773 K with a heating rate of 1 K/min . Spectra were taken after each heating step, i.e. the sample was cooled to RT and reheated. The adsorption of carbon dioxide was performed at RT after the last step (773 K), applying initial carbon dioxide pressures from 0.1 to 1.0 hPa . Spectra were taken 30 min after introduction of CO_2 .

2.3. Catalytic tests

The reaction was carried out in a fixed-bed once-through-plug-flow reactor made of quartz, operating at atmospheric pressure. The feed was a mixture of isopropanol and He obtained by passing He through liquid isopropanol held at a fixed temperature in a saturator. The reaction products were analyzed with on-line gas chromatography, using a Perkin-Elmer Auto System equipped a TCD and a FID detector connected in series. The amount of catalyst was 0.05 g with SiC added as a diluent, the partial pressure of

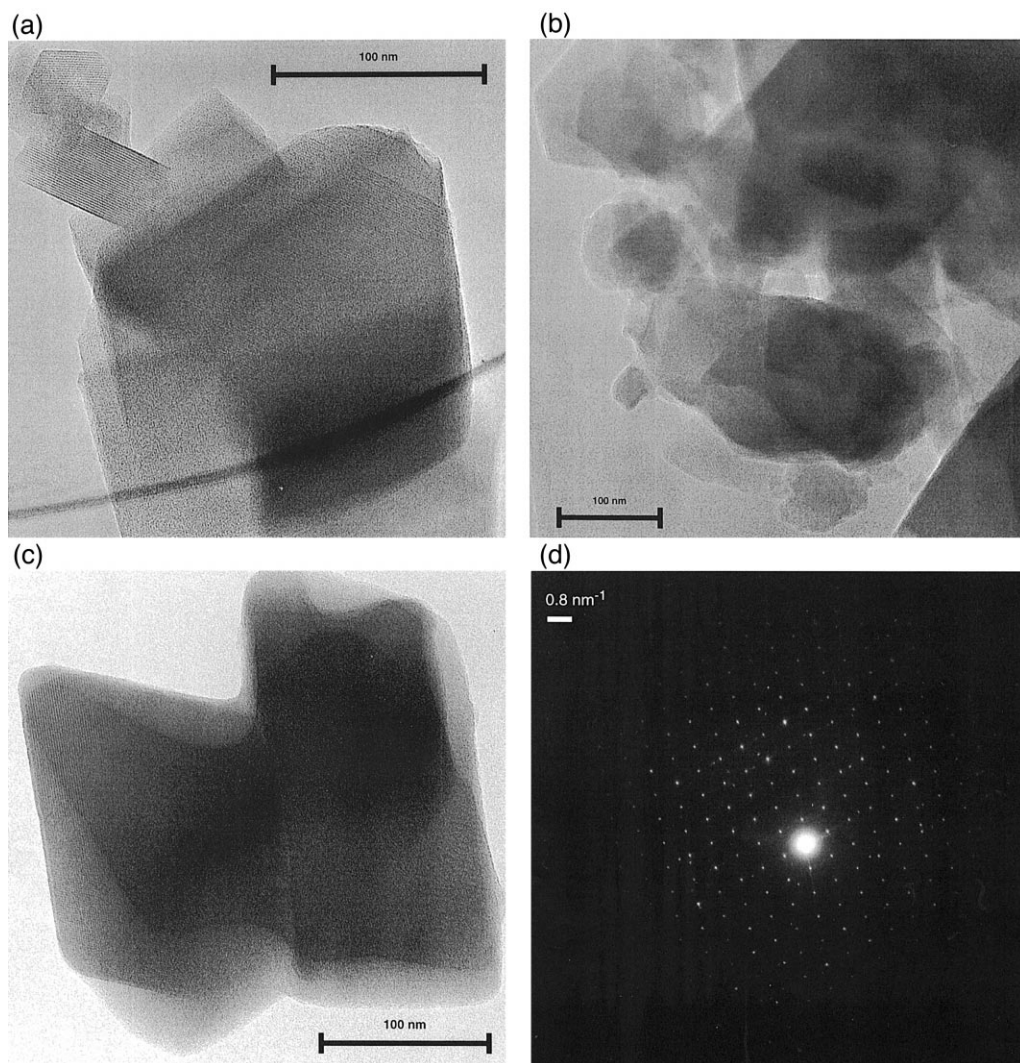


Fig. 4. TEM images of (a) NaY; (b) CsNaY; (c) CsY; (d) electron diffraction pattern of CsY; (e) CsNaX; and (f) $\text{Na}(\text{Ge})\text{X}$.

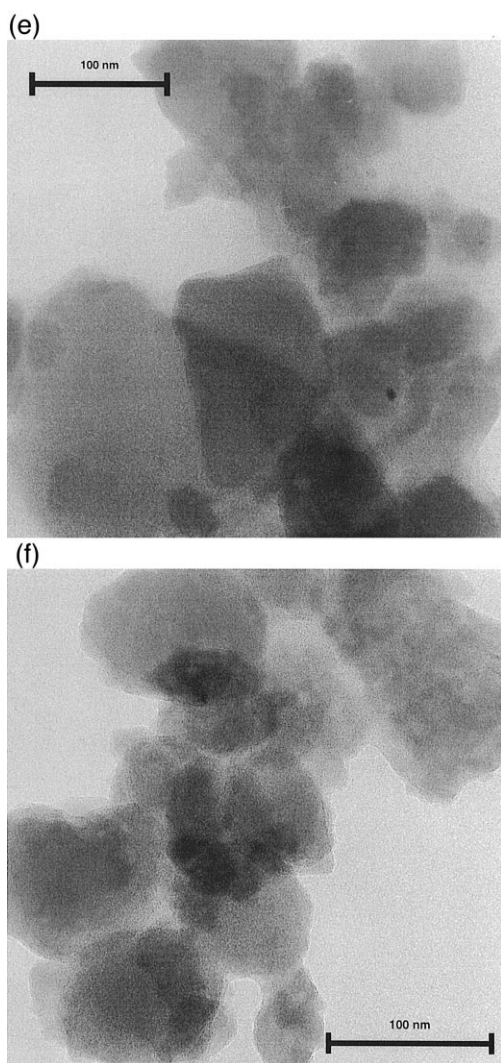


Fig. 4 (continued).

isopropanol in the feed was 5 kPa, and the total feed flow through the catalyst bed was 90 ml/min. Accounting for the water content of the catalyst samples (calculated from TG data in Table 1) and using the molecular weights given in Table 1, the inverse space velocities on a unit cell (u.c.) basis were as follows: NaY: 0.9 u.c.*s/molecule isopropanol; CsY: 1.2 u.c.*s/molecule; CsNaY, CsNaX, and Na(Ge)X: 0.7 u.c.*s/molecule. The reaction temperature was 623 K, and the time of reaction was 8 h. The catalysts, except Na(Ge)X, were pretreated in situ at 773 K (with a heating rate of 5 K/min), in a

flow of He (70 ml/min) for 2 h. The activation temperature for Na(Ge)X which is sensitive to temperatures above 673 K [36] was 623 K. Regeneration of the catalysts was either conducted in He (70 ml/min) or in 5% O₂ in He (100 ml/min), and lasted at least 2 h. The regeneration temperature was 773 K, in the case of Na(Ge)X, it was 623 K.

3. Results

3.1. Structure and composition

3.1.1. XRD

Diffractograms of all samples are shown in Figs. 1–3. The diffractograms of NaY, CsNaY, CsNaX (Fig. 1), and CsY-washed (Fig. 2) show solely reflections corresponding to faujasite. Cs-containing zeolites gave a different intensity distribution, as a consequence of the incorporation of Cs cations, which have different scattering properties. The diffractograms of the samples which had undergone cation exchange were characterized by an increased background (compared to the parent NaY), indicating an increased amorphous fraction in the material. The diffractogram of non-washed CsY showed additionally reflections of CsCl (Fig. 2). The average crystal size of CsCl, as determined from seven reflections with the Scherrer formula, was 55.0 nm. CsY was washed in order to remove the CsCl. The diffractogram recorded after the washing procedure (Fig. 2) did not show any reflections of CsCl but the background was increased, indicating a higher fraction of amorphous material. Three peaks in the diffractogram of the Na(Ge)X (Fig. 3) cannot be indexed with the faujasite structure. The peaks at $2\theta = 18.50^\circ$ and 18.79° can be assigned to Al(OH)₃, specifically to Bayerite and Nordstrandite, the peak at $2\theta = 37.50^\circ$ is assigned to GeO₂, specifically Argutite. Upon thermal treatment of the sample at 623 K (Fig. 3), the peaks at 18.50° , 18.79° disappeared, the peak at 37.50° gained in relative intensity, and the background increased.

XRD was also performed after reaction, including the regeneration attempts. Diffractograms of CsY and CsNaY were characterized by an increased background, indicating amorphous material, and peak

Table 2
CsY — composition from TEM/EDX analysis

Si/Al	Cs/Al	Cl/Al
2.46	0.85	0.06
2.44	1.61	0.27
2.61	1.95	0.19
2.53	0.96	0.20
2.64	1.49	0.19
2.53	1.72	0.27
2.59	0.93	0.07
2.53	1.21	0.12
2.56	1.24	0.14
2.43	1.14	0.08

broadening. NaY and CsNaX appeared more stable with regard to overall crystallinity, but the intensity distribution in the pattern of CsNaX was significantly altered after reaction. The diffractogram of Na(Ge)X suffered a strong increase in background and peak broadening already after treatment of the sample in He at 623 K (Fig. 3).

3.1.2. Electron microscopy

TEM images of NaY and CsY, presented in Fig. 4a and c, respectively, show well-defined crystals of

about 0.1–0.2 μm size. An electron diffraction pattern of CsY is shown in Fig. 4d. The morphology of CsNaY (Fig. 4b) and CsNaX (Fig. 4e) was different from that of NaY. The crystals were typically 0.1–0.2 μm large, and appeared to be of inferior quality with regard to the regularity of their shape. The Na(Ge)X sample consisted of about 0.1 μm , rather ill-defined crystals (Fig. 4f); additionally, diffuse islands of 0.2–0.3 μm size that contained only aluminum and oxygen were observed. With SEM–EDX, a rod-like crystal consisting of germanium and oxygen was detected (not shown) in the Na(Ge)X sample.

3.1.3. Chemical analysis (AAS and EDX)

Results of the chemical analysis are given in Table 1. NaY was found to have a molar ratio $n_{\text{Si}}/n_{\text{Al}} = 2.92$ by AAS, a value slightly higher than the value provided by the manufacturer. Cation exchange (CsY from NaY via NH_4Y), re-exchange (CsNaY from CsY), and washing (CsY-washed from CsY) did not significantly alter $n_{\text{Si}}/n_{\text{Al}}$. The $n_{\text{Cs}}/n_{\text{Al}}$ ratio in CsY was found to be 1.26 by AAS, reflecting the excess of Cs used in the preparation. The distribution of cesium was investigated by TEM–

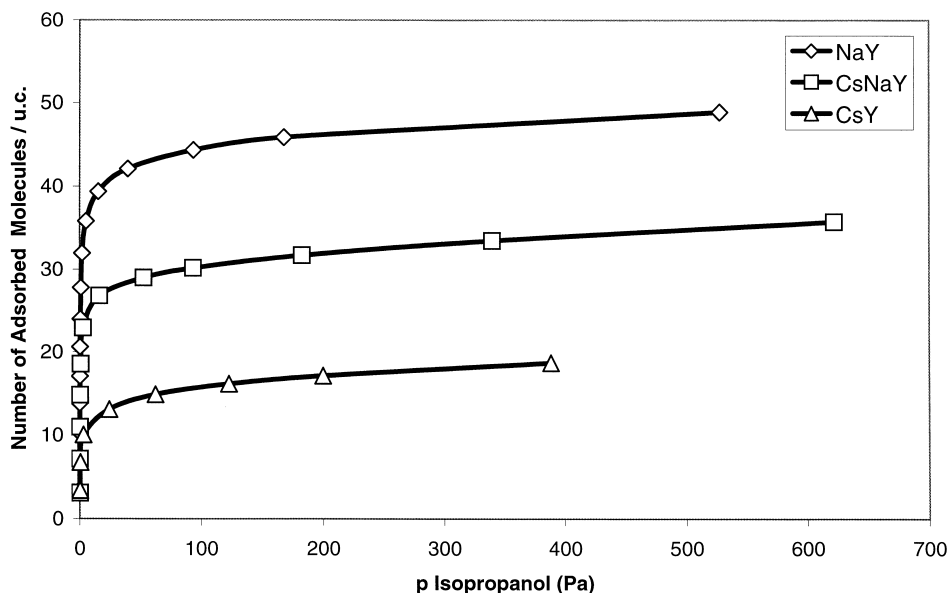


Fig. 5. Isopropanol adsorption isotherms of NaY, CsNaY, CsY, recorded at 353 K.

EDX, the data are summarized in Table 2. The cesium was found to be distributed inhomogeneously in CsY, $n_{\text{Cs}}/n_{\text{Al}}$ being in a range from 0.85 to 1.95. The average molar ratio $n_{\text{Cs}}/n_{\text{Al}}$ was 1.29, consistent with the AAS results. Wherever $n_{\text{Cs}}/n_{\text{Al}}$ exceeded 1, a considerable amount of Cl was detected (up to 10%), suggesting the presence of CsCl corresponding to the XRD results. In CsY-washed, $n_{\text{Cs}}/n_{\text{Al}}$ was determined to be 1.19 by AAS, and the decrease of the Cs content was confirmed by TEM-EDX. Chlorine was not detected with TEM-EDX in CsY-washed. The results indicate that excess CsCl was removed. In CsNaY, $n_{\text{Cs}}/n_{\text{Al}}$ (from AAS) was 0.79. Traces of chlorine were detected in this sample with TEM-EDX.

In CsNaX, $n_{\text{Si}}/n_{\text{Al}}$ as determined by AAS was 1.28, consistent with zeolite X. The Cs content, also from AAS, confirms an exchange ratio of ca. 50%. EDX of Na(Ge)X crystals gave $n_{\text{Ge}}/n_{\text{Al}} = 1.1$ and $n_{\text{Na}}/n_{\text{Al}} = 0.9$, close to the expected Na:Ge:Al = 1:1:1.

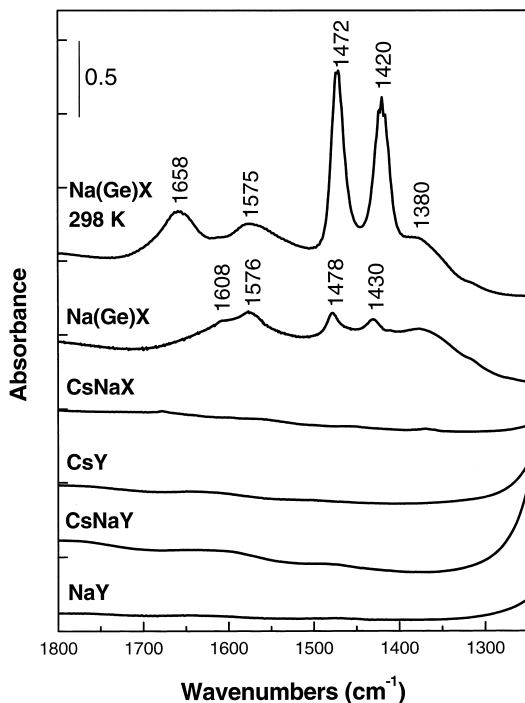


Fig. 6. Infrared spectra taken at RT after pretreatment in vacuum at 773 K or RT (Na(Ge)X) only.

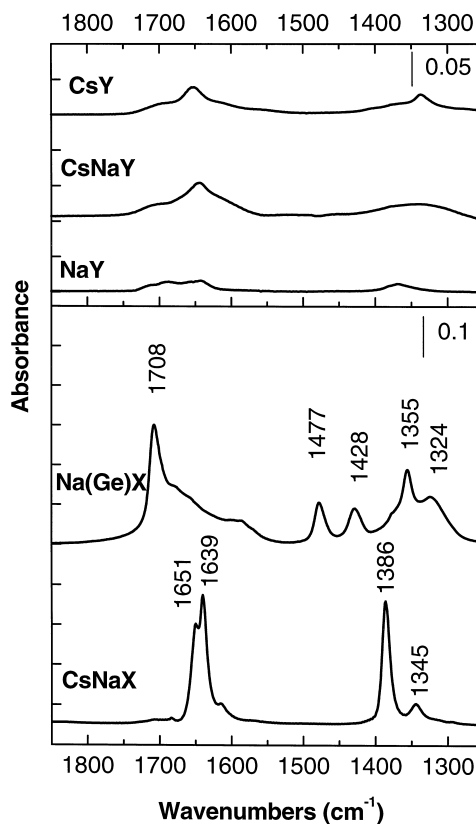


Fig. 7. Infrared spectra of the adsorption of CO_2 after pretreatment at 773 K. CO_2 partial pressure: 1 mbar; Na(Ge)X: 0.5 mbar. Spectrum of pretreated sample in vacuum subtracted.

3.2. TG, nitrogen sorption, and isopropanol sorption

TG measurements showed a weight loss in the temperature range from RT to 498 K for NaY, CsNaY, CsY and CsNaX; with the maxima in the DTG curves between 363 and 408 K. The DTG curve of Na(Ge)X showed two distinct maxima, at 288 K and at 523 K, the first weight loss corresponded to 13.3%, and the second weight loss which ended at 563 K corresponded to 4.2%. The sample continued losing weight up to 823 K, the total weight loss being 20%. Cumulative weight loss data are summarized in Table 1. The total weight loss decreased with increasing cesium content, as did the sorption capacity for nitrogen. The nitrogen sorption capacity of CsY was markedly increased after washing. Isopropanol adsorption isotherms at 353 K are

shown in Fig. 5. The amount of isopropanol adsorbed decreased in the order $\text{NaY} > \text{CsNaY} > \text{CsY}$.

3.3. Characterization by IR spectroscopy and carbon dioxide adsorption

3.3.1. Pretreatment

In the OH stretching mode region, the following bands were observed (not shown): all samples showed a broad absorption between 3650 and 3200 cm^{-1} , indicating physisorbed water. At RT, NaY showed a weak band at 3696 cm^{-1} . After treatment at 473 K , the broad water band was significantly decreased, and two bands at 3632 and 3541 cm^{-1} evolved. Both bands disappeared upon heating to 573 K . CsNaY was characterized by a band at 3739 cm^{-1} which was still visible after treatment at 773 K . CsY

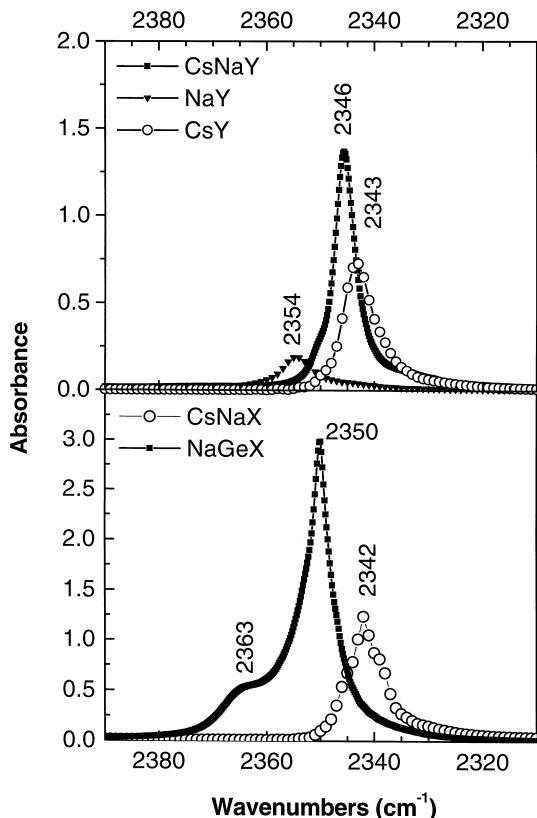


Fig. 8. Infrared spectra of the adsorption of CO_2 after pretreatment at 773 K . CO_2 partial pressure: 1 mbar ; $\text{Na}(\text{Ge})\text{X}$: 0.5 mbar . Spectrum of pretreated sample in vacuum subtracted.

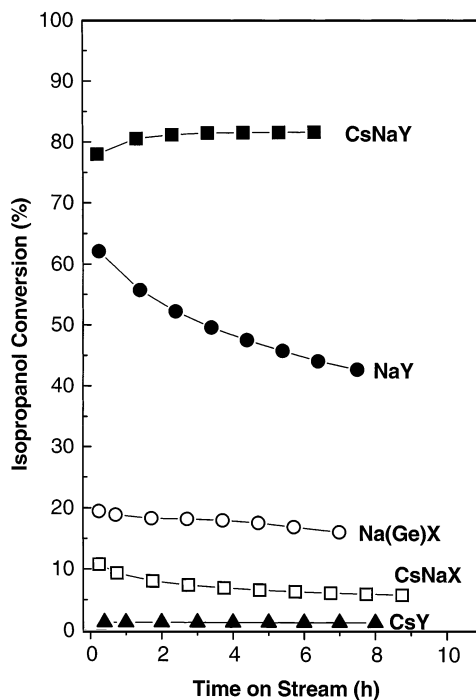


Fig. 9. Activity vs. time on stream. Catalyst mass = 50 mg ; $p(\text{isopropanol}) = 5\text{ kPa}$ in balance of He; total feed flow = 90 ml/min (NTP); reaction temperature = 623 K .

showed a very weak band at 3600 cm^{-1} after evacuation at RT which disappeared at 573 K . There were no bands in the spectrum between 4000 and 3000 cm^{-1} after heating CsY to 773 K . CsNaX featured two bands at 3712 and 3570 cm^{-1} which both were still observed after treatment at 773 K . At RT, $\text{Na}(\text{Ge})\text{X}$ had two pronounced bands at 3654 and 3615 cm^{-1} , and no bands in this region after being treated at 773 K . The region between 1800 and 1300 cm^{-1} is shown in Fig. 6. NaY, CsNaY, and CsY exhibited two weak bands, at ca. 1785 and 1475 cm^{-1} , and a stronger band at 1645 cm^{-1} , which decreased with increasing temperature. The spectrum of CsNaX that had been evacuated at RT, was characterized by bands at 1705 , 1642 , 1600 , 1586 (sh), 1466 , 1379 and 1335 cm^{-1} . After treatment at 773 K , two weak features at 1677 and 1370 cm^{-1} remained. $\text{Na}(\text{Ge})\text{X}$, treated in vacuum at RT overnight, showed strong absorption bands at approximately 1658 , 1575 , 1472 , 1420 and 1380 (sh) cm^{-1} . After treatment at 773 K , bands were ob-

served at 1608, 1576, 1478, 1430 and 1378 cm^{-1} . None of the spectra had bands between 2400 and 2300 cm^{-1} .

3.3.2. CO_2 adsorption

All spectra are presented as difference spectra with the spectrum of the pretreated sample subtracted. Spectra taken after adsorption of CO_2 at RT are shown in Figs. 7 and 8. The Y zeolites showed weak absorptions at the following positions: 1710, 1691, 1640, 1364 cm^{-1} (NaY); 1705, 1643, 1336 cm^{-1} (CsNaY); 1698, 1654, 1337 cm^{-1} (CsY). Strong absorption bands were observed at 2354 (NaY), 2346 (CsNaY), and 2343 cm^{-1} (CsY), Fig. 8.

After adsorption of CO_2 on CsNaX, intense bands at 1651, 1639, 1386 and 1345 cm^{-1} were detected (Fig. 7). The spectrum obtained after CO_2 adsorption on Na(Ge)X had bands at 1708, 1477, 1428, 1355

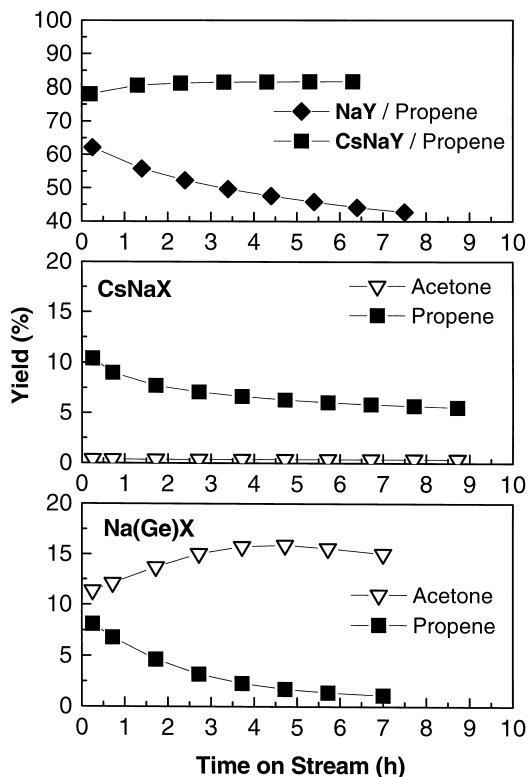


Fig. 10. Yield vs. time on stream. Catalyst mass = 50 mg; $p(\text{isopropanol}) = 5 \text{ kPa}$ in balance of He; total feed flow = 90 ml/min (NTP); reaction temperature = 623 K.

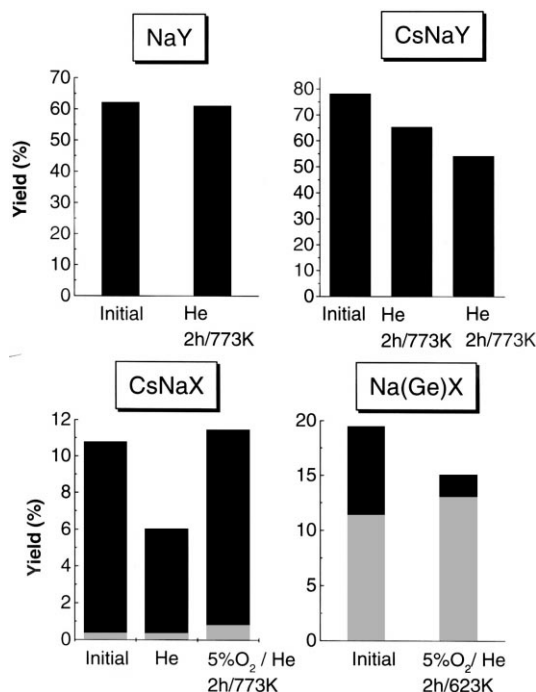


Fig. 11. Initial yields and yields after deactivation and subsequent reactivation. Catalyst mass = 50 mg; $p(\text{isopropanol}) = 5 \text{ kPa}$ in balance of He; and total feed flow = 90 ml/min (NTP). Reactivation in He, total feed flow = 70 ml/min; or 5% O_2 in He, total feed flow = 100 ml/min. Regeneration temperature = 773 K; Na(Ge)X: 623 K.

and 1324 cm^{-1} (Fig. 7). Strong absorption bands were observed at 2342 cm^{-1} (CsNaX), and at 2362 and 2350 cm^{-1} (Na(Ge)X), Fig. 8.

3.4. Catalytic tests / isopropanol conversion

The catalytic behavior of the different catalysts, i.e. the conversion of isopropanol, with time on stream is presented in Fig. 9. NaY, CsNaX, and Na(Ge)X showed a decrease of the conversion of isopropanol with reaction time. The conversion of isopropanol increased with reaction time in the case of the CsNaY, and non-washed CsY showed very little catalytic activity. The initial activities of the catalysts decreased in the order CsNaY > NaY > Na(Ge)X > CsNaX > CsY (non-washed).

Product distribution data from the first run, and after regeneration in He or in 5% O_2 /He, are presented in Figs. 10 and 11, respectively. CsY non-

washed is not discussed because of its low overall activity. Propene was the only product in the case of NaY and CsNaY. The yield of propene obtained with NaY decreased with time on stream (Fig. 10) and was completely regenerated by treatment of the catalyst in He at 773 K, shown in Fig. 11. The yield of propene increased with time on stream in the case of CsNaY (Fig. 10). Although CsNaY did not deactivate, it was subjected to the same “reactivation” procedure as the other catalysts; repeated treatment at 773 K in He resulted in a gradual decrease of the catalytic activity (Fig. 11) of CsNaY.

Propene and acetone were obtained using CsNaX as catalyst, but the yield of acetone was very low, i.e. $\sim 0.5\%$ (Fig. 10). Similar to NaY, the yield of propene decreased with reaction time while the acetone yield was almost constant (Fig. 10). It was not possible to regenerate the propene activity in He; 5% O₂ in He were necessary for a complete regeneration of the catalyst (Fig. 11). The yield of acetone was as high as 15% with Na(Ge)X as catalyst (Fig. 10). The yield of propene also decreased with reaction time; and the activity for propene formation could not be completely regenerated, not even in O₂.

4. Discussion

4.1. Crystallinity, composition, pore volume

4.1.1. CsY non-washed, from solid-state ion exchange

The maximum exchange degree obtainable with conventional ion exchange of NaY with Cs⁺ is about 70%, which has been explained by the inability of the Cs⁺ cations to enter the sodalite cages [38]. Through solid-state ion exchange with NH₄Y and CsCl, it is possible to obtain higher exchange degrees [39], even in a single step. IR spectra of our CsY show that both types of OH groups, indicated by high and low frequency bands, have reacted; and the adsorption of pyridine does not show any bands typical for Brønsted acidity; acidic OH groups are thus not present [39]. These data are consistent with complete cation exchange.

TEM shows that our CsY consists of well-defined crystals, and the X-ray diffractogram also demon-

strates that the structural integrity of the faujasite has been maintained through the ion exchange. However, the background in the diffractogram of CsY is increased in comparison to that of the starting material, which could either indicate an amorphization of the zeolite, or an X-ray amorphous fraction of CsCl as a result of the over-stoichiometric amount of CsCl used in the preparation.

Chemical analysis by AAS and by EDX data confirms the excess of Cs which is mainly present as chloride, in both dispersed and in crystalline form: crystals of 55-nm size were found with XRD that are too large to be inside the zeolite pore system. TEM-EDX of zeolite crystals shows chlorine wherever the Cs/Al ratio exceeded 1, indicating that amorphous CsCl is occluded in the zeolite. The formation of clathrates of faujasites with alkali metal salts through a thermal treatment has been described by Rabo and Kasai [40]. In their case, the materials were washed and all occluded salt was removed from the supercages; such clathrates were more stable at elevated temperatures and towards acids than the host zeolite. The excess CsCl thus serves not only as a driving force for the exchange reaction but it may help to retain the zeolite structure during the reaction.

A validation of the accessible pore space of CsY in comparison to NaY is difficult because the following points have to be accounted for: (i) the difference in the molecular weight of the u.c., (ii) the decrease in void volume through the more space consuming Cs in comparison to Na, (iii) the occlusion of CsCl which has a two-fold effect, i.e. the CsCl may block pores and it may account for about 5% of the weight of the sample, and (iv) some of the zeolite material may have become amorphous, assuming that the increased background in the diffractogram does not solely originate from amorphous CsCl. The sorption data are listed in Table 2 and presented in Fig. 5. The sorption capacity of CsY for nitrogen, isopropanol, and water, (assuming that the major fraction of the weight loss in the TG profile corresponds to water), is less than the sorption capacity of NaY.

4.1.2. CsY-washed

Successful removal of crystalline CsCl is demonstrated by the lack of CsCl reflections in the diffrac-

together of the washed material. The nitrogen adsorption on CsY substantially increases after washing, indicating that pores indeed were blocked by CsCl. The background in the diffractogram is increased and the lines are significantly broadened after washing, indicating further decomposition of the zeolite and the formation of amorphous species. Because the amount of occluded species decreases during washing, the amorphous species must originate from zeolite decomposition.

Excess cesium chloride that is necessary for complete cation exchange is demonstrated to block the pores and thus decreases the number of sites available for catalysis. The excess CsCl can be washed out, but washing appears to affect the structural integrity of the zeolite. Additionally, a strongly basic Cs salt solution must be used to avoid re-exchange of cesium cations for protons, but anions like hydroxide or carbonate can be introduced into the zeolite and because they are strongly basic, they can obscure the intrinsic basicity of the zeolite in a characterization or catalytic experiment.

4.1.3. Preparation of CsNaY and CsNaX by conventional ion exchange

CsNaY was prepared from CsY by a single exchange reaction in an aqueous NaCl solution. AAS results indicate that about 21% of the cesium cations were exchanged by sodium. The degree of exchange that can, in principal, be obtained by conventional ion exchange with Y zeolites is about 70% [38]. The sorption capacity of CsNaY is much lower than that of NaY which is consistent with partial exchange of Cs in the supercages. Had all cations except for the cations that are located in the sodalite cages or hexagonal prisms been replaced by sodium, the sorption capacities for nitrogen and isopropanol would be similar to those of NaY. The excess CsCl present in CsY is washed out in the preparation of CsNaY, the CsCl peaks cannot be found in the diffractogram anymore. A comparison of the diffractograms of CsNaY, CsY, and CsY-washed (Figs. 1,2) clearly shows that the crystallinity of the CsY sample is not affected by the treatment in the neutral NaCl solution, but it is strongly affected through the basic Cs₂CO₃ solution. These results indicate that cation exchange in strongly basic media can damage the

zeolite and the products of such exchanges should be analyzed for such damage.

When considering the exchange of Na cations in NaX with Cs cations, the Na ions can be classified, according to Sherry [38], into three groups: 43% of the Na cations, located in unidentified positions in the supercages, are readily exchanged, 38% of the Na cations that are in the supercages and near the windows to the hexagonal prisms (S II sites) can also be exchanged, the remaining 19% of the Na cations cannot be exchanged by a cation as large as Cs. The composition found for our CsNaX, i.e. somewhat above 50% of the cations are Cs, corresponds to a complete exchange of the first group of Na cations plus some additional exchange of the second group. Shepelev et al. [34] also obtained almost 50% exchange when preparing CsNaX from NaX, and in the hydrated state, Cs cations were located in the supercages at sites S III and S II. XRD and sorption capacity measurements confirm the structural integrity of the CsNaX sample.

4.1.4. Na(Ge)X

A diffractogram of Na(Ge)X was first published by Lerot et al. [36]. The three peaks at $2\theta = 18.50^\circ$, 18.79° , and 37.50° in our diffractogram are not present in Lerot's diffractogram, and these peaks cannot be indexed by the faujasite structure. The two peaks at 18.50° and 18.79° can be assigned to the main reflections of two different species of aluminum hydroxide, Al(OH)₃, i.e. Bayerite and Nordstrandite. Higher reflections are also present but overlap with reflections of Na(Ge)X. The peaks at 18.50° and 18.79° disappear upon thermal treatment of the sample at 623 K (Fig. 3), consistent with the decomposition of the hydroxides. The reflection at 37.50° matches exactly a reflection in the diffractogram of GeO₂, specifically Argutite, and the fit of the faujasite diffractogram could be significantly improved by leaving the strongest reflection of the GeO₂ at 28.65° out of the refinement. The results of the refinement are given in Table 3 and complete the data initially given by Lerot et al. [36]. The presence of aluminum hydroxides and germanium oxide can be explained with incomplete reaction during synthesis, in which Al is dissolved in NaOH, and GeO₂ is added. Al and Ge are employed in the synthesis in a stoichiometry

Table 3
Assignment of the observed reflections of Na(Ge)X

Observed 2θ (°)	<i>hkl</i>	Calculated 2θ (°)	Difference: observed–calculated (°)	Relative intensity (%)	Observed <i>d</i>
5.907	111	5.988	−0.0808	100.0	14.9494
9.754	220	9.786	−0.0320	15.4	9.0608
11.456	311	11.480	−0.0237	22.5	7.7178
15.098	331	15.106	−0.0086	21.4	5.8636
18.040	333	18.030	0.0103	8.7	4.9132
19.648	440	19.644	0.0041	10.5	4.5147
20.526	531	20.553	−0.0274	24.3	4.3235
21.991	620	21.990	0.0017	24.0	4.0386
22.822	533	22.810	0.0114	29.0	3.8935
24.153	444	24.119	0.0349	2.5	3.6817
24.878	551	24.873	0.0051	2.8	3.5762
26.084	642	26.084	0.0007	34.0	3.4134
26.787	553	26.786	0.0011	7.2	3.3254
29.656	660	29.651	0.0045	24.0	3.0100
30.281	555	30.277	0.0034	46.3	2.9493
31.300	840	31.295	0.0047	23.9	2.8555
31.892	753	31.892	−0.0002	5.6	2.8039
32.870	664	32.865	0.0054	24.5	2.7226
33.438	931	33.437	0.0010	21.1	2.6777
34.375	844	34.371	0.0044	6.8	2.6068
34.911	755	34.921	−0.0097	3.2	2.5680
35.826	862	35.821	0.0051	15.7	2.5045
36.743	666	36.527	−0.0534	19.5	2.4615
39.080	775	39.077	0.0025	16.8	2.3031
40.404	955	40.381	0.0226	19.4	2.2306
41.649	973	41.651	−0.0029	10.6	2.1668
42.417	884	42.430	−0.0130	13.6	2.1293
43.683	1064	43.651	0.0315	11.2	2.0705
44.098	975	44.102	−0.0040	13.9	2.0519

of 1:1 and it could be shown that Na(Ge)X is only stable with Al:Ge = 1:1 [36]. It can be speculated that the dissolution of GeO₂ was incomplete, and this resulted in an Al excess which formed hydroxide. The first weight loss observed in the TG curve of Na(Ge)X can be ascribed to the desorption of water from the zeolites pores. The second weight loss in the TG curve could be due to water loss during the transformation of Al(OH)₃ to AlO(OH); the transformation being consistent with the XRD results which do not show the reflections of the hydroxides anymore after treatment of Na(Ge)X at 623 K in He. The transition temperature for Al(OH)₃, which is of amphoteric nature, to AlO(OH) is in the range from 573 to 653 K; and at 673 K Al₂O₃ is formed [40]. GeO₂ was extremely difficult to find with the microscopic techniques applied, suggesting

it is a minor component in the system, and according to XRD highly crystalline and probably with a small surface area. Because GeO₂ has a rather acidic character [41], it is not to be expected to contribute to the formation of products of base catalysis, and thus would not falsely indicate the presence of basic sites.

4.2. Characterization by IR spectroscopy and CO₂ adsorption

4.2.1. CO₂ adsorption on cations

CO₂ has a kinetic diameter of 3.3 Å [42] and would not be expected to enter the sodalite cages which have six-ring openings of 2.2 Å in diameter [42]. Thus, CO₂ can only interact with the cations in the supercage. The weak interaction of CO₂ with

metal cations in the form of a $M^+ \dots O=C=O$ complex, leading to bands close to the antisymmetric stretching vibration of gas phase CO_2 (2349 cm^{-1}) was observed with all samples. Huber [43] investigated the adsorption of CO_2 on a series of cation exchanged Y zeolites. The antisymmetric stretching vibration of CO_2 weakly adsorbed on the cations was found at 2354 cm^{-1} for NaY and at 2346 cm^{-1} for CsY with a trend to decreasing wavenumbers with increasing cation size. Jacobs et al. [44] located the antisymmetric stretching vibration at 2357 cm^{-1} for CO_2 adsorbed on NaY. We observed bands at 2354 and 2343 cm^{-1} for NaY and CsY, respectively, and they are assigned to interaction of CO_2 with Na and Cs cations.

According to its chemical composition, CsNaY should have Cs and Na cations in the supercages. A migration of cations [33] during the dehydration prior to CO_2 adsorption or upon the CO_2 adsorption cannot be excluded and either Cs or Na cations may be located at S II or S III sites. The main fraction of CO_2 adsorbed on cations in CsNaY gives rise to a band at 2346 cm^{-1} ; there is a shoulder at about 2350 cm^{-1} . Neither of these bands has a position equal to the bands of CO_2 adsorbed on CsY or NaY. The position at 2346 cm^{-1} would suggest an interaction with Cs rather than with Na cations. The band at 2350 cm^{-1} is even more difficult to interpret; it could be an interaction with Na cations but it could also be due an interaction with Al cations. When adsorbing CO_2 on Al_2O_3 , Ramis et al. [45] observed a band at 2367 cm^{-1} , Little and Amberg [46] observed a band at 2350 cm^{-1} . An assignment to Al cations would mean that a substantial amount of extra-framework aluminum would have to be present, and we suggest that the band at 2350 cm^{-1} is due to an interaction of CO_2 with Na cations. Apparently, the presence of both Na and Cs affects the charge distribution inside the cage in such a way that the polarizing effect of Na and Cs on CO_2 is altered.

Jacobs et al. [47] adsorbed CO_2 on NaX and on CsNaX (54% Cs), and the bands of physisorbed CO_2 were found at 2357 and 2342 cm^{-1} . Huber [43] observed bands at the same positions when investigating NaX and CsNaX (51% Cs). Bertsch and Habgood [48], Kazansky et al. [49], and Ward and Habgood [50] investigated the adsorption of CO_2 on NaX, and they determined the position of the anti-

symmetric stretching of CO_2 to be 2355 [48], 2352 [49], and 2351 cm^{-1} [50]. We observed a band at 2342 cm^{-1} for the CsNaX, consistent with Jacob's and Huber's results, and suggesting that in our sample, mainly Cs cations are available in the supercages for interaction with the CO_2 as expected after conventional ion exchange. The band at 2342 cm^{-1} appears to have shoulders on both sides whose origin has not yet been determined. More than one band was observed when adsorbing CO_2 at increasing pressure on NaX [49,50], and it was proposed that this is due to different types of specifically adsorbed CO_2 [49], but splitting from the main band was much larger than in our case.

Upon CO_2 adsorption on Na(Ge)X, a band at 2350 cm^{-1} was produced, and this band is assigned to the adsorption of CO_2 on Na cations. The literature gives values between 2351 and 2355 cm^{-1} for adsorption of CO_2 on NaX [47–49], and a slight shift can be attributed to the different framework in our sample that has Ge in the place of Si and that may alter the polarizing ability of the Na cations. The shoulder at 2363 cm^{-1} is tentatively assigned to coordinatively unsaturated Al cations in the fraction of aluminum that did not react to form Na(Ge)X. The interaction of Al cations with CO_2 , depending on the environment, gives species at 2350 [46], 2360 [51] or 2367 [45] cm^{-1} . It cannot be excluded that the Ge atoms that did not react to Na(Ge)X also form linear adsorption complexes with CO_2 .

4.2.2. Carbonate formation

A number of species can be formed upon chemisorption of CO_2 on metal oxides [52,53], including monodentate, bidentate, and bridging bidentate carbonates; carboxylate, bicarbonate, and formate (the latter two require protons). In the IR spectrum, the carbonate species are characterized by band pairs (symmetric and antisymmetric stretching) which are located between 1250 and 1850 cm^{-1} . The splitting, which is typically $\sim 300\text{ cm}^{-1}$ for bidentate carbonates and $\sim 100\text{ cm}^{-1}$ for monodentate carbonates, is a measure of the basicity of the substrate oxygen, where the basicity increases with decreasing splitting [54]. If the CO_2 molecule is sufficiently bent upon physisorption, the symmetric stretching mode (1388 cm^{-1}) can become IR active,

and would give an additional band in this spectroscopic region [44,49].

The weak bands of CO₂ adsorbed on NaY, CsNaY, and CsY (Fig. 7) can be assigned to bidentate structures. The two bands at 1654 and 1337 cm⁻¹ observed for CsY are similar to the observations of Huber [43]. CO₂ adsorption does not indicate pronounced basicity in any of these materials.

CO₂ adsorption on CsNaX leads to bands at 1651, 1639, 1615, 1386 and 1345 cm⁻¹ which is consistent with the results obtained by Huber [43]. Jacobs et al. [47] observed a band pair, i.e. bands which show a similar behavior upon heating or evacuation with a constant intensity ratio and are thus assigned to one species, at 1650 and 1385 cm⁻¹, consistent with our work, but also a pair at 1690 and 1345 cm⁻¹ where we only observed the band 1345 cm⁻¹. Huber [43] also observed an intense band at 1674 cm⁻¹ with a cesium hydroxide impregnated CsNaX; the band was assigned to the presence of cesium oxide clusters. We did not detect this band in any of our cesium containing samples and can thus exclude the presence of cesium oxide species.

The spectra taken after CO₂ adsorption on Na(Ge)X not only show the bidentate species but also a band pair at 1477 and 1428 cm⁻¹; these bands are not removed upon evacuation, and their intensity is almost equal. Bertsch and Habgood [48] observed a band pair at 1485 and 1425 cm⁻¹ when adsorbing CO₂ on NaX and proposed that the small splitting indicates an almost symmetrical carbonate structure. Jacobs et al. [47] suggested that Na cations in S III positions are involved in stabilizing this “true” carbonate structure. The observation of this structure is restricted to NaX; it is not formed with LiX, KX [48], or RbX [47], presumably because the electrostatic field is either too low (K, Rb) or too much shielded (Li), and it is not formed with NaY, probably because of a lack of charge density on the oxygens. The band pair at 1477 and 1428 cm⁻¹ is thus interpreted as representative of a monodentate carbonate species, and the shift in comparison to the species formed on NaX is most likely due to the effect of Ge on the framework polarity. The spectra taken of Na(Ge)X after evacuation and heating, and without deliberate CO₂ adsorption, Fig. 6, are similar to the spectra obtained by Lerot et al. [55]. The

bands at 1472 and 1420 cm⁻¹ clearly indicate the presence of the monodentate symmetrical carbonate, providing evidence that Na(Ge)X reacts with CO₂ from the environment.

From investigation of CO₂ adsorption by IR spectroscopy, the following ranking of basicity evolves: Y zeolites (not basic) < CsNaX (mildly basic) < Na(Ge)X (basic).

4.3. Catalytic tests / isopropanol conversion

4.3.1. Overall activity

The initial activities of the catalysts decrease in the order CsNaY > NaY > GeX > CsNaX > CsY (Fig. 9). On a basis of u.c., the contact times were about the same for CsNaY, CsNaX, and GeX, and they were slightly higher for NaY and CsY. The order of activity of the alkali metal cation exchanged Y zeolites is not a simple function of the accessible pore space, or the isopropanol sorption capacity. Specifically, CsNaY is more active than NaY, and CsY is almost inactive but the pore volume and the isopropanol adsorption decrease in the order NaY > CsNaY > CsY, and CsY still has significant sorption capacity. The adsorption of isopropanol was performed at 353 K and may not reflect the scenario under catalytic conditions. Nevertheless, the reasons for the high activity of CsNaY remain unclear. The low activity of CsY may be explained by (i) a steric hindrance of the interaction of isopropanol with the active sites due to the larger Cs cation size (radius 1.67 Å) in comparison to the Na cation (radius 0.99 Å), (ii) the presence of pore blocking CsCl, or (iii) simply the lack of catalytically active sites. Our CsY does not have Brønsted acid sites [39], the Lewis acidity of Cs cations is negligible, and basic sites could not be detected when CO₂ was adsorbed. Only impurities could thus account for the activity. Weitkamp et al. [56] found CsY (100%) to behave like a solid acid catalyst, and NMR revealed residual Brønsted acid sites due to incomplete reaction during the exchange procedure.

CsNaX and Na(Ge)X were less active than NaY and CsNaY but more active than CsY. There is again no simple relation between activity and sorption data, suggesting a difference in the nature of active sites on these catalysts. Indeed, the product distributions of (i) NaY and CsNaY, (ii) CsNaX, and (iii)

Na(Ge)X are entirely different which supports the idea of the presence of various types of active sites.

4.3.2. Selectivity and regeneration

The possible reaction pathways of isopropanol on metal oxides have been investigated by Gervasini et al. [35], with the following conclusions. Acetone, the dehydrogenation product, is only formed from isopropanol when the catalyst provides strongly basic Lewis sites. Propene, the dehydration product, can be formed through different mechanisms that require either (i) strongly acidic Brønsted or Lewis sites, or (ii) Lewis base and Lewis acid sites, both of medium strength, or (iii) strongly basic Lewis sites and weakly acidic Lewis sites. The selectivity of the reaction depends strongly on the reaction temperature, with the formation of propene being favored at higher reaction temperatures [57].

Only propene was formed in the presence of NaY and CsNaY. These results are consistent with the findings of Weitkamp et al. [56] who did not find any selectivity for acetone with NaY, with the findings of Jacobs and Uytterhoeven [13] who found acetone selectivity for NaY only in the presence of cationic impurities such as Fe, and with the findings of Hathaway and Davis [20] who found no acetone selectivity for unrinsed and only little acetone selectivity for rinsed CsNaY made from NaY and CsCl. The yield of propene decreased with time on stream for NaY, but initially increased to a constant level for CsNaY. Yashima et al. [19] who investigated the conversion of isopropanol in the presence of various alkali metal exchanged X and Y zeolites, also observed a decrease in the dehydration activity within the first few hours on stream. We could easily regenerate NaY in He at 773 K, and we propose that deactivation is due to contamination with light hydrocarbon side products which are easily desorbed. CsNaY did not deactivate during the reaction but was subjected to “regeneration” anyway. It was less active after treatment in He, and continued to lose activity with repeated treatments in He. XRD analysis following the series of reaction and regeneration cycles showed an increasing background and line broadening, indicating that the decrease in activity caused by heating in He was due to disintegration of the zeolite.

CsNaX, like NaY and CsNaY, produced propene, and this reaction pathway was subject to deactivation, consistent with the observations by Yashima et al. [19]. The sites on CsNaX yielding propene were not regenerated as easily as those of NaY, oxygen was necessary for recovery of propene formation. It appears that some coke is formed perhaps due to polymerization of propene. Small amounts of acetone are also formed in the presence of CsNaX, and the sites responsible for this product do not deactivate with time on stream. The different deactivation behavior indicates that acetone and propene are formed at different sites. If coke was responsible for deactivation of the sites that form propene, it does not affect the sites that form acetone, further indicating that the two different sites are not in close proximity to each other. Our CsNaX can be compared to other partially exchanged zeolites that were also made through exchange with chlorides and are free of occluded oxides and hydroxides. Yashima et al. [19] and Berkani et al. [58] also found CsNaX active for dehydrogenation of alcohols. Yashima, reacting isopropanol, observed a constant acetone yield after a short induction period, and Su and Barthomeuf [10] used CsNaX successfully for *N*-alkylation. All these reactions indicate the presence of basic sites. Yashima et al. [3] ascribed the low activity of CsNaX in the side chain alkylation of toluene that was found against a trend among the alkali metal cations to partial destruction of the crystallinity of CsNaX. We could not find evidence for structural degradation of CsNaX in the diffractograms; however, there were changes in the intensity distribution that may suggest cation migration.

The propene yield for Na(Ge)X was nearly the same as that for CsNaX, but the acetone yield was significantly higher, i.e. 10–15% vs. < 1%. Lerot et al. [55] investigated the reaction of isopropanol in the presence of Na(Ge)X and found that propene was the major product at 473 and 573 K, and that the selectivity towards acetone was < 5% at 573 K. We found a higher selectivity towards acetone than Lerot et al. which may be explained by the difference in reaction temperature (623 K in our case) because acetone has a high affinity to Na(Ge)X at 573 K [55] and may thus not desorb. Evidence for the presence of basic sites on Na(Ge)X includes CO₂ adsorption results ([55], this work), pyrrole adsorption results

[21], and catalytic data [14,15] obtained from Knoevenagel condensations. The formation of acetone is thus consistent with previous observations. Poncelet and Dubru [59] could not find any acid sites by pyridine adsorption and IR spectroscopy but they point out that acid sites are not totally absent because, e.g. *n*-butene can be isomerized. However, a contribution of the oxidic Al impurities in our sample to the product distribution cannot entirely be ruled out, particularly Al cations could function as strongly acidic Lewis sites.

The structural integrity of Na(Ge)X suffered already during heating to 623 K in He (Fig. 3), confirming the observations of Lerot et al. [36] who reasoned [55] that Na(Ge)X is inherently unstable because Ge favors six-fold over four-fold coordination. Lerot et al. [55] also suggested that the strong interaction of Na(Ge)X with CO₂ involves an expansion of the Ge coordination. It is thus not surprising that Na(Ge)X cannot be entirely reactivated, and the deactivation is probably at least in part due to disintegration.

In summary, the yield of acetone decreases in the order Na(Ge)X \gg CsNaX > CsNaY = NaY = 0, which is in agreement with the order of basicity obtained by IR spectroscopy and the order reported in the literature.

5. Conclusions

Careful analysis with XRD, microscopic techniques, and sorption of various molecules was extremely helpful in interpreting the catalytic performance of several modified faujasite-type zeolites. XRD allowed the confirmation of structural integrity, after individual preparation steps (exchange, washing procedures) as well as after reaction. TEM-EDX and SEM-EDX are excellent complementary methods to bulk chemical analysis, which alone appears not always sufficient to follow cation exchange reactions. The spatial resolution together with the elemental analysis allowed the identification of impurities and provided information on the homogeneity of the samples.

To avoid the introduction of a basic cation that would obscure the determination of the intrinsic

basicity of the zeolite, alkali metal chlorides were used for all exchange reactions. It was possible to prepare Cs exchanged Y zeolite by solid-state ion exchange with an exchange degree of nearly 100%. The structural integrity of the zeolite was maintained during the exchange but the pore system was partially blocked by excess CsCl from the preparation. It may be possible to optimize the exchange to avoid such blockage but the catalytic results so far obtained are not promising. NaY and CsNaY (made from CsY with NaCl) were active for isopropanol conversion but propene was the only product. Consistent with the catalytic behavior, no strongly basic sites could be detected with CO₂ adsorption and IR spectroscopy.

CsNaX was also active for isopropanol conversion but propene was the major product and only very little acetone was formed. Only germanium faujasite Na(Ge)X, with Ge replacing Si in the framework, exhibited pronounced selectivity towards acetone which is indicative of the presence of stronger basic sites. These results were also consistent with CO₂ adsorption; CO₂ formed an almost symmetrical carbonate ion on Na(Ge)X, indicative of basic sites. Na(Ge)X was contaminated with extra-framework Al and Ge species from incomplete reaction during synthesis, and diffractograms taken after thermal treatment of Na(Ge)X at 623 K showed its partial disintegration.

The yield of propene decreased with time on stream for NaY, CsNaX, and Na(Ge)X. Activity for propene formation could be regenerated in He (NaY), in 5% O₂/He (CsNaX), or not at all (Na(Ge)X). Reasons for the deactivation may be the formation of different species of coke, and/or disintegration of the zeolite. The formation of acetone remained constant with time on stream for Na(Ge)X, indicating that acetone and propene are formed on different sites.

In summary, the composition of the framework (X vs. Y, Ge in place of Si) appeared to have a stronger influence on the basicity than the charge balancing cations; CsNaX and Na(Ge)X both underwent structural changes during activation/catalysis. Characterization with a number of techniques is necessary to determine the result of ion exchange reactions, i.e. desired effects and side effects, otherwise trace impurities, pore blocking, or partial decomposi-

tion may lead to misinterpretation of catalytic results. Future work should thus include extensive and systematic preparative efforts.

Acknowledgements

The authors would like to thank Gabriella Pál-Borbély for assistance with the sample preparation, Joachim Schütze for performing the N₂ adsorption experiments, Richard Schumacher for performing the isopropanol adsorption experiments, Gisela Lorenz for performing the AAS measurements, Gisela Weinberg for performing the SEM experiments, and Yuji Uchida for obtaining the electron diffraction patterns. Robert Schlögl is thanked for support and valuable discussions. Funding from the EU Human Capital and Mobility — Scientific and Technical Cooperation Network (CHRX-CT94-0477) is gratefully acknowledged.

References

- [1] D. Barthomeuf, Catal. Rev. — Sci. Eng. 38 (1996) 521.
- [2] M.L. Unland, G.E. Barker, US Patents 4140726 and 4115424.
- [3] T. Yashima, K. Sato, T. Hayasaka, N. Hara, J. Catal. 26 (1972) 303.
- [4] J. Engelhardt, J. Szanyi, J. Valyon, J. Catal. 107 (1987) 296.
- [5] N. Giordano, L. Pino, S. Cavallaro, P. Vitarelli, B.S. Rao, Zeolites 7 (1987) 131.
- [6] S.T. King, J.M. Garces, J. Catal. 104 (1987) 59.
- [7] K. Arishtirova, P. Kovacheva, N. Davidova, Appl. Catal., A 167 (1998) 271.
- [8] P. Kovacheva, K. Arishtirova, N. Davidova, Appl. Catal., A 178 (1999) 111.
- [9] P.R. Hari Prasad Rao, P. Massiani, D. Barthomeuf, Catal. Lett. 31 (1995) 115.
- [10] B.L. Su, D. Barthomeuf, Appl. Catal., A 124 (1995) 73.
- [11] E.J. Doskocil, R.J. Davis, J. Catal. 188 (1999) 353.
- [12] P.A. Jacobs, M. Tielen, J.B. Uytterhoeven, J. Catal. 50 (1977) 98.
- [13] P.A. Jacobs, J.B. Uytterhoeven, J. Catal. 50 (1977) 109.
- [14] A. Corma, R.M. Martín-Aranda, F. Sánchez, J. Catal. 126 (1990) 192.
- [15] A. Corma, R.M. Martín-Aranda, F. Sánchez, in: M. Guisnet et al. (Eds.), Heterogeneous Catalysis and Fine Chemicals II, Elsevier, Amsterdam, p. 503.
- [16] S.V. Bordewekar, R.J. Davis, J. Catal. 189 (2000) 79.
- [17] J.C. Kim, H.-X. Li, C.-Y. Chen, M.E. Davis, Microporous Mater. 2 (1994) 413.
- [18] M.D. Sefcik, J. Am. Chem. Soc. 101 (1979) 2164.
- [19] T. Yashima, H. Suzuki, N. Hara, J. Catal. 33 (1974) 486.
- [20] P.E. Hathaway, M.E. Davis, J. Catal. 116 (1989) 263.
- [21] P.O. Scokart, P.G. Rouxhet, Bull. Soc. Chim. Belg. 90 (1981) 983.
- [22] M. Huang, S. Kaliaguine, J. Chem. Soc., Faraday Trans. 88 (1992) 751.
- [23] M. Huang, A. Adnot, S. Kaliaguine, J. Catal. 137 (1992) 322.
- [24] M. Laspéras, H. Cambon, D. Brunel, I. Rodriguez, P. Geneste, Microporous Mater. 1 (1993) 343.
- [25] M. Laspéras, H. Cambon, D. Brunel, I. Rodriguez, P. Geneste, Microporous Mater. 7 (1996) 61.
- [26] D. Barthomeuf, J. Phys. Chem. 88 (1984) 42.
- [27] J. Xie, M. Huang, S. Kaliaguine, Appl. Surf. Sci. 115 (1997) 157.
- [28] Y. Okamoto, M. Ogawa, A. Maezawa, T. Imanaka, J. Catal. 112 (1988) 427.
- [29] R. Heidler, G.O.A. Janssens, W.J. Mortier, R.A. Schoonheydt, J. Phys. Chem. 100 (1996) 19728.
- [30] H.K. Beyer, H.G. Karge, G. Borbély, Zeolites 8 (1988) 79.
- [31] G. Borbély, H.K. Beyer, L. Radics, P. Sándor, H.G. Karge, Zeolites 9 (1989) 428.
- [32] H.G. Karge, H.K. Beyer, in: P.A. Jacobs, N.I. Jaeger, L. Kubelková, B. Wichterlová (Eds.), Stud. Surf. Sci. Catal. vol. 69 Elsevier, Amsterdam, 1991, p. 43.
- [33] H. Koller, B. Burger, A.M. Schneider, G. Engelhardt, J. Weitkamp, Microporous Mater. 5 (1995) 219.
- [34] Yu.F. Shepelev, I.K. Butikova, Yu.I. Smolin, Zeolites 11 (1991) 287.
- [35] A. Gervasini, J. Fenyvesi, A. Auroux, Catal. Lett. 43 (1997) 219.
- [36] L. Lerot, G. Poncelet, J.J. Fripiat, Mater. Res. Bull. 9 (1974) 979.
- [37] R. Schumacher, Dissertation, Berlin 1997.
- [38] H.S. Sherry, J. Phys. Chem. 70 (1966) 1158.
- [39] C. Jia, G. Pal-Borbély, E. Coker, U. Härtel, F.C. Jentoft, R. Schlögl, H.G. Karge, International Symposium on Acid-Base Catalysis III, Rolduc, The Netherlands, April 20–24, 1997.
- [40] J.A. Rabo, P.H. Kasai, Prog. Solid State Chem. 9 (1975) 1.
- [41] A.F. Holleman, E. Wiberg, Lehrbuch der Anorganischen Chemie, 91.-100. Auflage, Walter de Gruyter, Berlin, 1985.
- [42] D.W. Breck, Zeolite Molecular Sieves, Wiley, New York, 1974, p. 636.
- [43] S. Huber, Dissertation, Ludwig-Maximilians-Universität, Munich, 1997.
- [44] P.A. Jacobs, F.H. van Cauwelaert, E.F. Vansant, J.B. Uytterhoeven, J. Chem. Soc., Faraday Trans. 69 (1973) 1056.
- [45] G. Ramis, G. Busca, V. Lorenzelli, Mater. Chem. Phys. 29 (1991) 425.
- [46] L.H. Little, C.H. Amberg, Can. J. Chem. 40 (1962) 1957.
- [47] P.A. Jacobs, F.H. van Cauwelaert, E.F. Vansant, J. Chem. Soc., Faraday Trans. 69 (1973) 2130.
- [48] L. Bertsch, H.W. Habgood, J. Phys. Chem. 67 (1963) 1621.
- [49] V.B. Kazansky, V.Yu. Borovkov, A.I. Serykh, M. Bulow, Phys. Chem. Chem. Phys. 1 (1999) 3701.
- [50] J.W. Ward, H.W. Habgood, J. Phys. Chem. 70 (1966) 1178.

- [51] C. Morterra, G. Ghiotti, F. Boccuzzi, S. Coluccia, *J. Catal.* 51 (1978) 299.
- [52] A.M. Turek, I.E. Wachs, E. DeCanio, *J. Phys. Chem.* 96 (1992) 5000, and references therein.
- [53] J.C. Lavalley, *Catal. Today* 27 (1996) 377.
- [54] A.A. Davydov, M.L. Shepot'ko, A.A. Budneva, *Kinet. Catal.* 35 (1994) 272.
- [55] L. Lerot, G. Poncelet, M.L. Dubru, J.J. Fripiat, *J. Catal.* 37 (1975) 396.
- [56] J. Weitkamp, S. Ernst, M. Hunger, T. Röser, S. Huber, U.A. Schubert, P. Thomasson, H. Knözinger, in: J.W. Hightower, W.N. Delgass, E. Iglesia, A.T. Bell (Eds.), *Stud. Surf. Sci. Catal.* vol. 101 Elsevier, Amsterdam, 1996, p. 731.
- [57] A. Ouqour, G. Coudurier, J.C. Vedrine, *J. Chem. Soc., Faraday Trans.* 89 (1993) 3151.
- [58] M. Berkani, J.L. Lemberton, M. Marczewski, G. Perot, *Catal. Lett.* 31 (1995) 405.
- [59] G. Poncelet, M.L. Dubru, *J. Catal.* 52 (1978) 321.